

# CRITICAL ASSESSMENT OF RANS THERMAL TURBULENCE MODELS FOR LOW PRANDTL NUMBER FLOWS

***J. Schmitt<sup>1</sup>, J. Neuhäuser<sup>1</sup>, D. Gatti<sup>1</sup>, B. Frohnäpfel<sup>1</sup> and L. Marocco<sup>2</sup>***

<sup>1</sup> *Institute of Fluid Mechanics, Karlsruhe Institute of Technology, Germany*

<sup>2</sup> *Department of Energy, Politecnico di Milano, Italy*

*jonathan.schmitt@kit.edu*

## Abstract

In turbulent flows of low Prandtl number fluids, the similarity between turbulent momentum and heat transfer is impaired. Models, which are based on this similarity, cannot be used for RANS simulations of small Prandtl number flows, which then require the adoption of more complex thermal turbulence models for their correct description.

In this work, the Kays correlation, a  $k$ - $\epsilon$ - $k_\theta$ - $\epsilon_\theta$  model, a  $k$ - $\Omega$ - $k_\theta$ - $\Omega_\theta$  model and an algebraic turbulent heat flux model with the associated  $k$ - $\epsilon$  turbulence model were implemented in OPENFOAM. The comparative investigation of the models and the verification of the reproducibility of results from other authors were carried out on the cases of flows through a channel and over a backward-facing step. The  $k$ - $\epsilon$ - $k_\theta$ - $\epsilon_\theta$  model and the Kays correlation in combination with the  $k$ - $\omega$  SST model show promising results for potential use in RANS simulations of low Prandtl number flows. For all other model combinations, no conclusive evaluation of the applicability for flows with small Prandtl numbers can be made due to the lack of reproducibility or low numerical robustness.

## 1 Introduction

Simulations based on the Reynolds-Averaged Navier–Stokes Equations (RANS) are the industry standard in the design of systems involving turbulent flows, or in the setup of more accurate scale-resolving simulations, such as Detached Eddy Simulation (DES) and Large Eddy Simulations (LES). In the RANS context, thermal problems pose additional challenges, since both the Reynolds stress tensor  $\bar{u}_i' u_j'$  and the turbulent heat flux  $\bar{u}_i' T'$  need to be consistently modeled. The corresponding simplified averaged temperature equation, which needs to be solved, is as follows:

$$\frac{\partial \bar{T}}{\partial t} + \bar{u}_i \frac{\partial \bar{T}}{\partial x_i} = \frac{\partial}{\partial x_i} \left( \alpha \frac{\partial \bar{T}}{\partial x_i} \right) - \frac{\partial}{\partial x_i} \left( \bar{u}_i' T' \right) \quad (1)$$

where  $u_i$  is a velocity component along the Cartesian directions  $x_i$ ,  $T$  the temperature and  $\alpha$  the thermal diffusivity. The superscript  $(\cdot)'$  indicates a turbulent fluctuation and an average value is denoted with  $(\cdot)$ . The

most widespread turbulent thermal diffusivity models approximate the turbulent heat flux through the Simple Gradient Diffusion Hypothesis (SGDH) via a scalar turbulent diffusivity  $\alpha_t$  as follows:

$$\bar{u}_i' T' = -\alpha_t \frac{\partial \bar{T}}{\partial x_i}. \quad (2)$$

The modeling problem boils thus down to determining the turbulent Prandtl number

$$Pr_t = \frac{\nu_t}{\alpha_t}, \quad (3)$$

i.e. the ratio between the already modeled turbulent eddy viscosity  $\nu_t$  and the turbulent thermal diffusivity has to be determined.  $Pr_t$  is the turbulent equivalent of the Prandtl number  $Pr$  itself, which relates the molecular fluid viscosity and thermal diffusivity. For fluids with  $Pr \approx 1$ , such as air, it is customary to assume the so-called Reynolds analogy, i.e. that the similarity between the molecular diffusivities also holds for the turbulent ones, yielding:

$$Pr_t \approx 1. \quad (4)$$

As Kays (1994) reports,  $Pr_t$  is a constant in the log region for high values of  $Pr$ . Therefore this simple modeling approach may be effective also for fluids with  $Pr \gg 1$ , but it fails for fluids with  $Pr \ll 1$ , where the similarity between turbulent momentum and heat transfer is impaired. This limitation therefore excludes for example the correct modeling of liquid metal flows.

For the RANS momentum equations, few models are well established in practice and broad experience regarding their capabilities and applicability is available. In contrast, while various more advanced thermal models - i.e. not resorting to the SGDH - have been proposed, there is less consensus on the performance of these models. As a result, advanced thermal turbulence models have not been systematically compared yet, let alone using the same spatial and temporal discretisation, and simulation framework.

Therefore, the present work aims at critically assessing the most common and most promising thermal turbulence models for forced convection in low

Prandtl number flows, by comparing their predictive performance for two benchmark cases for which more accurate simulations exist. The comparison is performed utilising the same simulation framework, by implementing the models in the open-source simulation suite OPENFOAM (Weller et al., 1998).

## 2 Models

## Overview

Most of the assessed thermal turbulence models are calibrated to a specific momentum turbulence model. Table 1 provides an overview of the assessed model combinations along with relevant literature references. The models MM, DAVIA, SHAMS-KE and SHAMS-EBRSM solve transport equations for additional thermal variables, whereby half of the temperature variance is defined as

$$k_\theta := \frac{1}{2} \overline{T' T'} \quad (5)$$

and  $\epsilon_\theta$  is the corresponding dissipation rate. For the definitions of the logarithmic variables  $\Omega$  and  $\Omega_\theta$  the reader is referred to Da Vià et al. (2016). The tested models include those based on the SGDH as well as algebraic heat flux models (AHFM). Most of the models have been implemented in OPENFOAM as part of this study, with the exception of the  $k-\omega$  SST and EBRSM models, for which the existing OPENFOAM implementations have been used. In comparison to the standard values of OPENFOAM v2212 the following model coefficients of the EBRSM were changed to  $A_1 = 0.1$  and  $C_l = 0.122$ . Motivated by the work of Kays (1994),  $Pr_t = 0.85$  is used for the Reynolds analogy model.

## Implementation differences

Special attention is given to ensuring correct model implementations, particularly concerning governing equations, model coefficients and functions. More significant changes compared to the formulas in the literature specified in Table 1 are summarized in the following.

The implementation of the turbulence model LIEN is primarily based on the equations given in Shams et al. (2014). However, the function  $F_2$  follows Lien et al. (1996) and thus has different signs than those given in Shams et al. (2014). It is given by:

$$F_2 = \left(1 - Ce^{-R_t^2}\right) \quad (6)$$

with  $R_t = k^2/(\nu\epsilon)$  and  $C = 0.3$ . In addition, the so-called Yap correction, whose concept is described in Yap (1987), was added to the transport equation of the dissipation rate of turbulent kinetic energy. The reason for adding the correction term is that it is mentioned in subsequent publications, such as the article by Shams (2018).

The implementation of the  $k_\theta$ - $\epsilon_\theta$  model is primarily based on Manservisi and Menghini (2014),

whereby for the model coefficients  $C_\theta$ ,  $Pr_{t\infty}$ ,  $C_\gamma$ ,  $\sigma_{k\theta}$ ,  $\sigma_{\epsilon\theta}$ ,  $C_{p1}$ ,  $C_{d1}$ ,  $C_{p2}$  and the functions  $f_{1\theta}$ ,  $f_{2a\theta}$ ,  $f_{2b\theta}$  and  $C_{d2}$  formulas from Manservisi and Menghini (2015) are used.

The  $k\theta$ - $\Omega_\theta$  model implementation differs from the formulas provided by Da Vià et al. (2016) by the following. In the transport equation of  $\Omega_\theta$  the sink term  $-C_\mu(C_{d1} - 1)e^{\Omega_\theta}$  has the additional factor  $C_\mu$ . Following Da Vià and Manservisi (2019)  $B_{1\theta}$  was set to 1/1.33. For  $C_{d2}$  the function and for  $C_{p2}$  the value by Manservisi and Menghini (2015) were taken instead of the formulas provided by Da Vià et al. (2016).

### 3 Case configurations

The models are validated and their predictive capabilities are assessed based on two benchmark flow cases, for which accurate Direct Numerical Simulations (DNS) are available.

First, a turbulent channel flow with prescribed mean wall heat flux is simulated at values of friction Reynolds number  $Re_\tau$  between 180 and 640 and  $Pr = 0.025$ , for which DNS data by Kawamura (2004) are available.

Second, a backward facing step (BFS) with expansion ratio  $ER = 1.5$ , bulk Reynolds number (defined by mean velocity and inlet channel height)  $Re_b = 9610$ , and  $Pr = 0.0088$ , for which DNS data by Niemann and Fröhlich (2016) exist. The flow configuration, shown in Figure 1, features a partially heated bottom wall. The geometry measurements were selected as  $l_{in}/l_{step} = 2$ ,  $l_{out}/l_{step} = 10$  and  $l_{top}/l_{step} = 32$ . This flow case is utilized to assess model accuracy in a more complex scenario with separation and recirculation zones, in which near-wall turbulence is not fully-developed and homogeneous along the wall-parallel directions.

For both setups the so called mixed-type boundary condition are applied to the temperature related variables, where the boundary conditions for  $k_\theta$ ,  $\epsilon_\theta$  and  $\Omega_\theta$  can be found e.g. in the articles of Manservisi and Menghini (2014) and Da Vià et al. (2016).

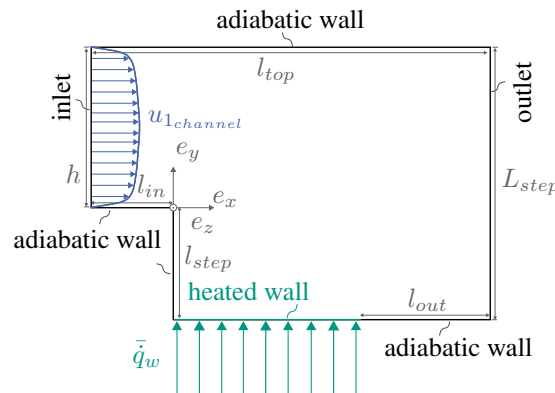


Figure 1: Schematic (not to scale) of the flow geometry over a backward-facing step.  $u_{1,\text{channel}}$  symbolically represents the prescribed inlet conditions of a turbulent channel flow.

Table 1: Overview of the selected combinations of momentum and thermal turbulence model, as well as literature references for each of them. Each model combination is given an acronym.

Mom. Model	Thermal Model			Abbreviation
$k-\omega$ SST	Menter et al. (2003)	Kays correlation	Kays (1994)	KWSST-KAYS
$k-\epsilon$ (AKN)	Abe et al. (1994)	Reynolds analogy		AKN-RA
$k-\epsilon$ (AKN)	Abe et al. (1994)	$k_\theta-\epsilon_\theta$	Manservisi and Menghini (2014)	MM
$k-\Omega$ (KLW)	Da Vià et al. (2016)	$k_\theta-\Omega_\theta$	Da Vià et al. (2016)	DAVIA
$k-\epsilon$ (LIEN)	Lien et al. (1996)	AHFM-NRG	Shams et al. (2014)	SHAMS-KE
EBRSM	Manceau (2015)	AHFM-NRG	Shams and De Santis (2019)	SHAMS-EBRSM

## 4 Results and discussion

The models are evaluated based on the reproducibility of literature data, their complexity, their ability to accurately capture key thermal transport phenomena and thus reproduce DNS results.

### Channel flow

As can be seen from the results at  $Re_\tau = 395$  for the velocity  $\bar{u}_1$  in viscous units in Figure 2, all turbulence models reproduce the DNS results with sufficient accuracy. The KLW and LIEN models show small deviations from the results in the comparative literature, which are the articles by Da Vià et al. (2016) and Shams et al. (2014).

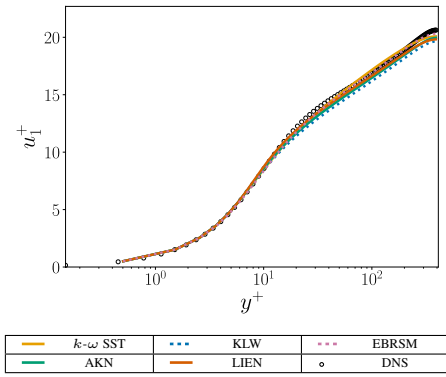


Figure 2: Profiles of the mean velocity in the main flow direction in wall units. Channel flow at  $Re_\tau = 395$ . DNS data from Kawamura (2004).

In Figure 3 (a) the temperature  $\theta = \bar{T}_{wall} - \bar{T}$ , in (b)  $\bar{u}_2' \bar{T}'$  and in (c) the root of the temperature variance  $\sqrt{\bar{T}' \bar{T}'}$  are each shown in wall units for the simulations at  $Re_\tau = 395$ .

The Reynolds analogy in combination with the AKN model overestimates the negative turbulent heat flux in the wall normal direction and consequently the temperature  $\theta^+$  is underestimated. Since the Reynolds analogy model is designed for fluids with  $Pr \approx 1$ , for which a similarity may exist, the turbulent contribution to the heat transfer process is incorrectly overestimated for small Prandtl numbers, as expected. The combination of the Kays correlation and the  $k-\omega$  SST

model, on the other hand, can approximately reproduce the mean temperature profile of the DNS data. As can be seen in Figure 3 (b), the results for the turbulent heat flux of MM and the DNS are similar. Consequently, this model combination can also reproduce the profile of  $\theta^+$  of the DNS well. In contrast to the Reynolds analogy and the Kays correlation, all other thermal turbulence models in the study solve a modeled transport equation of  $k_\theta$ . Its results in the form of the root of the temperature variance in wall units are shown in Figure 3 (c). The model combination MM reproduces the standard deviation of the DNS temperature with good approximation. Apart from minor deviations, DAVIA also captures the mean and the standard deviation of the DNS temperature.

The model SHAMS-KE overestimates  $\theta^+$ . Figure 3 (c) also shows that this implemented model combination cannot be used to predict the temperature variance of the DNS data. The results for  $\theta^+$  and  $\bar{T}' \bar{T}'^+$  do not reproduce the data of Shams et al. (2014). However, for the combination SHAMS-EBRSM the results of Shams and De Santis (2019) are reproduced.

In order to compare the results at different Reynolds numbers, the relative deviation of the Nusselt number from DNS reference data is shown in Figure 4. The Nusselt number for the present case is given as:

$$Nu = \frac{2\delta \bar{q}_w}{\theta_b \lambda_F} \quad (7)$$

where  $\delta$  is the half channel height,  $\theta_b$  the mixed mean temperature,  $\bar{q}_w$  the mean wall-normal heat flux and  $\lambda_F$  the thermal conductivity.

The model combinations KWSST-KAYS, MM, DAVIA and SHAMS-EBRSM can predict the Nusselt numbers of the DNS for  $Re_\tau \in \{180, 395, 640\}$  at  $Pr = 0.025$  with a relative deviation of less than 7.22%. AKN-RA overestimates  $Nu$  by up to 23.64% and is therefore not suitable for correctly representing the heat transfer in the present case. Similarly, one of the implemented variants of the AHFM-NRG model, the SHAMS-KE, cannot reproduce the DNS data for  $Re_\tau = 395$  and  $Re_\tau = 640$ .

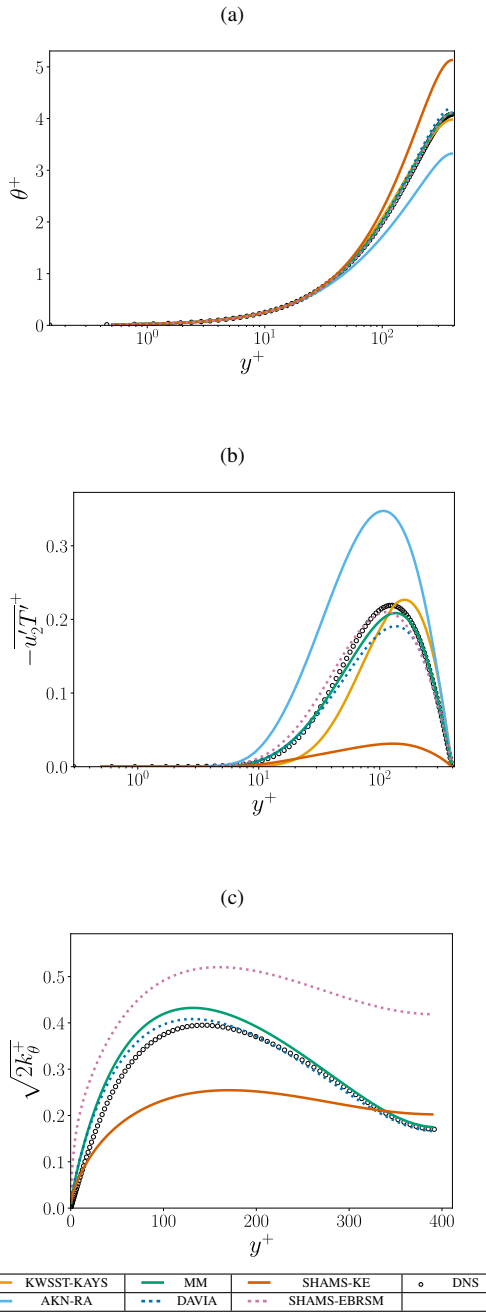


Figure 3: Profiles of the following variables in wall units: (a) mean temperature, (b) negative turbulent heat flux in the wall normal direction and (c) standard deviation of temperature ( $\sqrt{\bar{T}' T'} = \sqrt{2k_\theta}$ ). Channel flow at  $Re_\tau = 395$  and  $Pr = 0.025$ . DNS data from Kawamura (2004).

### Backward-facing step

Because no turbulent converged solution could be generated for SHAMS-EBRSM applied to the configuration of the backward-facing step shown in Figure 1, this combination is excluded from the following discussion. Although it was possible to determine a turbulent converged solution for the momentum-related variables using the KLW model, all simulations with the DAVIA model led to divergence. Therefore, only

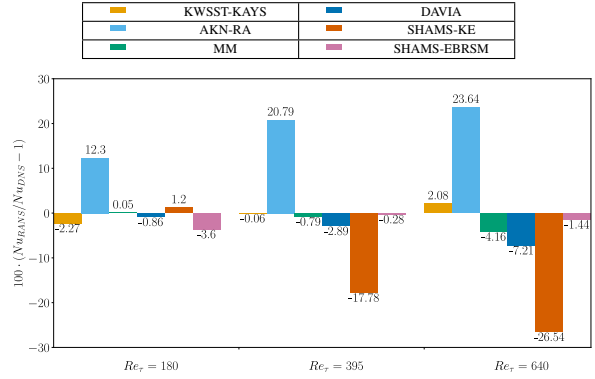


Figure 4: Relative deviation of the Nusselt numbers of the RANS simulations ( $Nu_{RANS}$ ) from the results of the DNS ( $Nu_{DNS}$ ). Channel flow at  $Pr = 0.025$ . DNS data from Kawamura (2004).

the results of the KLW turbulence model are presented in the following.

The friction coefficient

$$c_f = \frac{\tau_w}{\frac{1}{2} \rho u_b^2} \quad (8)$$

is illustrated in Figure 5. In Equation (8)  $\tau_w$  is the wall shear stress,  $\rho$  the density and  $u_b$  the bulk velocity at the inlet. The results of the momentum-related variables for the  $k-\omega$  SST and AKN models correspond to those of Schumm et al. (2015). Similarly, the results of the LIEN model reproduce the results of De Santis and Shams (2018). Thus a detailed description of the results for the friction coefficient and the velocity field is omitted and reference is made instead to Schumm et al. (2015) and De Santis and Shams (2018). The results of the combination MM for the mean of the dimensionless over-temperature reproduce the results of Schumm et al. (2015), so reference is made to their explanations for a detailed interpretation. Analogous to the channel flow, the temperature-related results of SHAMS-KE do not match the data of the reference, which is the article by De Santis and Shams (2018) in the case of the BFS. For this reason, these results will not be discussed further.

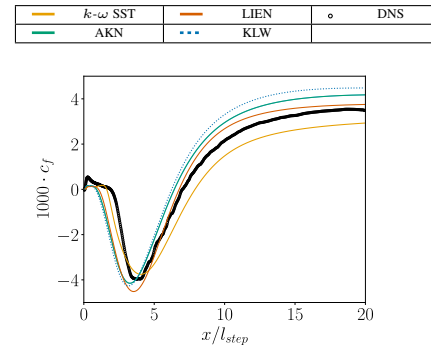


Figure 5: Friction coefficient  $c_f$  along the heated wall section. DNS data from Niemann and Fröhlich (2016).

For investigating the mean wall temperature, the local Nusselt number  $Nu_x$  along the heated wall is shown in Figure 6. Here, the definition of  $Nu_x$  is the same as in Schumm et al. (2016). For the present case  $Nu_x$  is the reciprocal of the mean over-temperature at the wall. Similar to the channel flow, the Reynolds analogy model is unsuitable for predicting  $Nu_x$  for the BFS. MM mostly yields an overestimated Nusselt number in the region over which the DNS recirculation area is formed, but downstream it best reflects  $Nu_x$  compared to the other models. In the area near the step, KWSST-KAYS best reproduces the results for  $Nu_x$  of the DNS compared to all other models. However, downstream, this model overestimates the mean wall temperature, which may be partially due to the overprediction of the reattachment length. As the thermal model is dependent on the accurate prediction of the momentum-based variables, the turbulence model and the thermal model must be regarded as a combination. Since the numerically simple and robust Kays correlation does not necessarily have to be used with the  $k$ - $\omega$  SST model, a turbulence model that better predicts the flow field might improve accuracy.

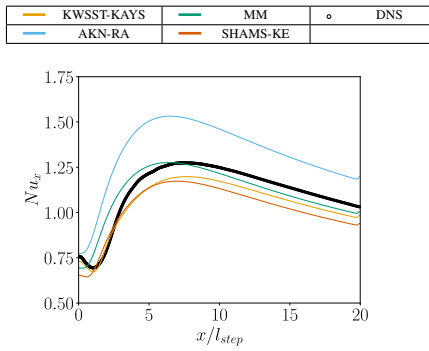


Figure 6: Local Nusselt number  $Nu_x$  along the heated wall section. DNS data from Niemann and Fröhlich (2016).

## 5 Conclusions

In this work, various RANS-based models for predicting heat transfer in turbulent flows of fluids with low Prandtl numbers were investigated and partially implemented in OPENFOAM. The KWSST-KAYS and MM models deliver promising results in the cases examined. As expected, the Reynolds analogy model is not a suitable thermal turbulence model for flows of low Prandtl number fluids. For the DAVIA and SHAMS-EBRSM models, the simulation settings should be further varied in the future to obtain a converged solution. Furthermore, the model description of the SHAMS-KE model and its implementation should be further investigated.

## Acknowledgments

We greatly acknowledge the support by the German Research Foundation (DFG) under grant number 423710075.

## References

Abe, K., Kondoh, T. and Nagano, Y. (1994), A new turbulence model for predicting fluid flow and heat transfer in separating and reattaching flows - I. Flow field calculations, *Int. J. Heat and Mass Transf.*, Vol. 37, pp. 139–151.

Da Vià, R. and Manservisi, S. (2019), Numerical simulation of forced and mixed convection turbulent liquid sodium flow over a vertical backward facing step with a four parameter turbulence model, *Int. J. Heat and Mass Transf.*, Vol. 135, pp. 591–603.

Da Vià, R., Manservisi, S. and Menghini, F. (2016), A  $k$ - $\Omega$ - $k_\theta$ - $\Omega_\theta$  four parameter logarithmic turbulence model for liquid metals, *Int. J. Heat Mass Transf.*, Vol. 101, pp. 1030–1041.

De Santis, A. and Shams, A. (2018), Application of an algebraic turbulent heat flux model to a backward facing step flow at low Prandtl number, *Annals Nucl. Ener.*, Vol. 117, pp. 32–44.

Kawamura, H. (2004), *Numerical Simulation Data Base for Turbulent Channel Flow with Heat Transfer* [Data set], Tokyo University of Science, <https://www.rs.tus.ac.jp/t2lab/db/>.

Kays, W.M. (1994), Turbulent Prandtl Number - Where Are We?, *J. Heat Transf.*, Vol. 116, pp. 284–295.

Lien, F.S., Chen, W.L. and Leschziner, M.A. (1996), Low-Reynolds-number eddy-viscosity modelling based on non-linear stress-strain/vorticity relations, in Rodi and Bergeles (Eds.), *Engineering Turbulence Modelling and Measurements 3*, pp. 91–100, Elsevier.

Manceau, R. (2015), Recent progress in the development of the Elliptic Blending Reynolds-stress model, *Int. J. Heat Fluid Flow*, Vol. 51, pp. 195–220.

Manservisi, S. and Menghini, F. (2014), A CFD four parameter heat transfer turbulence model for engineering applications in heavy liquid metals, *Int. J. Heat Mass Transf.*, Vol. 69, pp. 312–326.

Manservisi, S. and Menghini, F. (2015), CFD simulations in heavy liquid metal flows for square lattice bare rod bundle geometries with a four parameter heat transfer turbulence model, *Nucl. Eng. Des.*, Vol. 295, pp. 251–260.

Menter, F.R., Kuntz, M. and Langtry, R. (2003), Ten Years of Industrial Experience with the SST Turbulence Model, in K. Hanjalić, Y. Nagano and M. Tummers (Eds.), *Turbulence, heat and mass transfer 4*, pp. 625–632, Begell House, Inc., New York.

Niemann, M. and Fröhlich, J. (2016), Buoyancy-affected backward-facing step flow with heat transfer at low Prandtl number, *Int. J. Heat and Mass Transf.*, Vol. 101, pp. 1237–1250.

Schumm, T., Frohnapfel, B. and Marocco, L. (2016), Numerical simulation of the turbulent convective buoyant flow of sodium over a backward-facing step, *Journal of Physics: Conference Series*, Vol. 745, p. 32051.

Schumm, T., Niemann, M., Magagnato, F. et al. (2015), Numerical prediction of heat transfer in liquid metal applications, in *Proceedings of the Eighth International Symposium On Turbulence Heat and Mass Transfer*, pp. 263–266.

Shams, A. (2018), Towards the accurate numerical prediction of thermal hydraulic phenomena in corium pools, *Annals of Nuclear Energy*, Vol. 117, pp. 234–246.

Shams, A. and De Santis, A. (2019), Towards the accurate prediction of the turbulent flow and heat transfer in low-Prandtl fluids, *Int. J. Heat and Mass Transf.*, Vol. 130, pp. 290–303.

Shams, A., Roelofs, F., Baglietto, E. et al. (2014), Assessment and calibration of an algebraic turbulent heat flux model for low-Prandtl fluids, *Int. J. Heat Mass Transf.*, Vol. 79, pp. 589–601.

Weller, H.G., Tabor, G., Jasak, H. et al. (1998), A tensorial approach to computational continuum mechanics using object-oriented techniques, *Comput. Phys.*, Vol. 12, pp. 620–631.

Yap, C.R. (1987), *Turbulent heat and momentum transfer in recirculating and impinging flows* (Publication No. 30279570) [Dissertation, The University of Manchester], ProQuest Dissertations Publishing.